

# Polarization of $\Lambda(1405)$ in the $\gamma p \rightarrow K^+ \pi \Sigma$ reaction

Ke Wang<sup>1</sup> and Bo-Chao Liu<sup>1,\*</sup>

<sup>1</sup>*School of Physics, Xi'an Jiaotong University, Xi'an, Shannxi 710049, China*

In this paper, we study the polarization of the  $\Lambda(1405)$  in the  $\gamma p \rightarrow K^+ \pi \Sigma$  reaction within an effective Lagrangian approach and isobar model. In our model, the  $\Lambda(1405)$  is excited through the t-channel  $K/K^*$  exchanges and u-channel hyperon exchange. Compared to previous studies, we also include the contribution from a contact term, which is necessary for our model to interpret the polarization of the  $\Lambda(1405)$ . In addition, we also discuss the possibility to verify the proposed two-pole structure of the  $\Lambda(1405)$  using the polarization data. We find that the polarization of the  $\Lambda(1405)$  or the polarization of the final  $\Sigma$  in this reaction is sensitive to the invariant mass  $M_{\pi\Sigma}$ . Thus the measurement of the dependence of the  $\Lambda(1405)$  polarization on the  $M_{\pi\Sigma}$  can offer valuable information about the pole structure of the  $\Lambda(1405)$ .

PACS numbers:

## INTRODUCTION

The structure and properties of the  $\Lambda(1405)$  is an interesting and important topic in hadron physics, which has attracted a lot of interest since its existence was predicted[1, 2]. Due to the attractive interaction between antikaons and nucleons, the  $\Lambda(1405)$  may be a quasibound molecular state of the  $\bar{K}N$  system. While, in the conventional quark model the  $\Lambda(1405)$  was also described as a  $p$ -wave state of three-quark system[3]. In the 1990's, the  $\Lambda(1405)$  was investigated within the Chiral Unitary approach, and it was found that the  $\Lambda(1405)$  could be dynamically generated, i.e. appearing as poles in the amplitude, through the SU(3) dynamics[4]. An interesting finding in this approach is that, in contrast to the conventional opinions, the observed bump of the  $\Lambda(1405)$  is in fact due to two poles in the amplitude. This finding was confirmed by a series of further theoretical studies[5–7]. The possibility of existing of two poles in the  $\Lambda(1405)$  region has stimulated a lot of further efforts to explore the nature of the  $\Lambda(1405)$ . Unfortunately, up to now there is still no final conclusion about whether the two-pole structure exists or not. It is fair to say that we still do not understand the nature of the  $\Lambda(1405)$  very well.

Among the various studies on the  $\Lambda(1405)$ , we are interested in the  $\Lambda(1405)$  production in the photo induced process. In Refs.[8, 9], the study of the  $\Lambda(1405)$  production in the  $\gamma p \rightarrow K^+ \pi \Sigma$  reaction was reported by the CLAS Collaboration. They measured the angular distribution of the final  $K^+$  and the invariant mass spectrum of  $\pi \Sigma$ , which offer a good opportunity for studying the properties of the  $\Lambda(1405)$  and verifying its possible two-pole structure. These data were analyzed in Refs.[10–13]. However, it seems current data cannot offer enough constraints on the model. Therefore, it is still not possible to draw the conclusion about the two-pole conjecture. Besides the measurement of the angular distribution and the

invariant mass spectrum, some progress was also made in identifying the quantum numbers of this resonance. In Ref.[14], the CLAS Collaboration reported their results on determining the quantum numbers of the  $\Lambda(1405)$ , which confirmed the quantum numbers  $J^P$  of the  $\Lambda(1405)$  is  $\frac{1}{2}^-$ . What makes this experiment interesting for us is the idea of the measurement of the  $\Lambda(1405)$  polarization in their work. In order to measure the spin and parity of the  $\Lambda(1405)$ , the  $\Lambda(1405)$  is assumed to be produced polarized in this reaction. Even though the clarifying of the mechanism for the  $\Lambda(1405)$  polarization in this reaction is not necessary for the purpose of measuring its quantum numbers, it is certainly interesting and important for understanding the reaction mechanisms. Since in the experimental analysis[14] the  $\Lambda(1405)$  is treated as a single resonance, it will also be interesting to discuss the possible effects if considering the two-pole structure of the  $\Lambda(1405)$ . In previous studies, these issues were not considered. So the main goal of the present work is twofold. First, we hope to discuss the mechanism for the polarization of the  $\Lambda(1405)$  in this reaction. In fact, we find the polarization data can offer further constraints on the model, which are helpful for understanding the reaction mechanisms. Second, we hope to discuss the effects due to the pole structure of the  $\Lambda(1405)$  on the  $\Lambda(1405)$  polarization. This issue is interesting because it may offer a new way to verify the two-pole picture of the  $\Lambda(1405)$ . Since we hope to concentrate on the mechanism for the  $\Lambda(1405)$  polarization in the present work, we will only consider the experimental data at the center-of-mass energies ranging from 2.3 GeV to 2.8 GeV, where the s-channel nucleon resonance contribution is small[15] and the polarization of the  $\Lambda(1405)$  was measured.

This paper is organized as follows. In Sec. II, the theoretical framework and ingredients are presented. In Sec. III, the numerical results are presented with some discussions. Finally, the paper ends with a short summary in Sec. IV.

---

\*Electronic address: liubc@xjtu.edu.cn

## MODEL AND INGREDIENTS

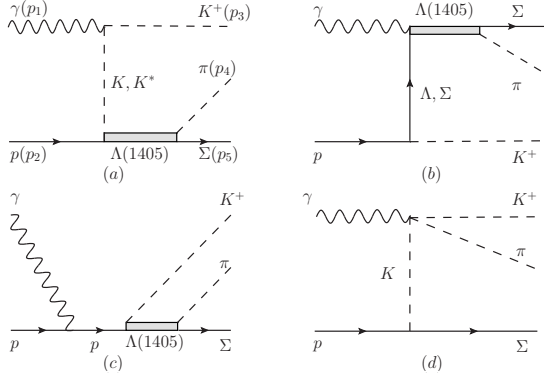


FIG. 1: Feynman diagrams for the  $\gamma p \rightarrow K^+ \pi \Sigma$  reaction.

In the present work, we study the  $\gamma p \rightarrow K^+ \pi \Sigma$  reaction at the c.m. energies ranging from 2.3 GeV to 2.8 GeV within an effective Lagrangian approach and isobar model. As mentioned in Sec. I, at these energies the  $s$ -channel nucleon resonance contribution can be ignored. To describe this reaction, we consider the Feynman diagrams shown in Fig.1, which include the pseudoscalar and vector meson exchanges in the  $t$ -channel, the hyperon exchange in the  $u$ -channel, nucleon pole term in the  $s$ -channel and a contact term. To evaluate these Feynman diagrams, the effective Lagrangian densities for the interaction vertices are needed. For the electromagnetic interaction vertices, we have the interaction Lagrangian densities[15, 16]:

$$\mathcal{L}_{\gamma KK} = -ie_K [K^\dagger (\partial_\mu K) - (\partial_\mu K^\dagger) K] A^\mu, \quad (1)$$

$$\mathcal{L}_{\gamma KK^*} = g_{\gamma KK^*} \varepsilon^{\mu\nu\alpha\beta} \partial_\mu A_\nu [(\partial_\alpha K_\beta^{*-}) K^+ + K^- (\partial_\alpha K_\beta^{*+})], \quad (2)$$

$$\mathcal{L}_{\gamma NN} = -\bar{N} \left[ e_N \gamma_\mu - \frac{e k_N}{2M_N} \sigma_{\mu\nu} \partial^\nu \right] A^\mu N, \quad (3)$$

$$\mathcal{L}_{\gamma Y \Lambda^*} = \frac{e \mu_{\Lambda^* Y}}{2M_N} \bar{Y} \gamma_5 \sigma_{\mu\nu} \partial^\nu A^\mu \Lambda^* + \text{H.c.}, \quad (4)$$

$$\mathcal{L}_C = -\frac{i e g_c}{8\pi^2 F_\pi^3} \varepsilon^{\mu\nu\alpha\beta} F_{\mu\nu} \pi \partial_\alpha K \partial_\beta \bar{K}, \quad (5)$$

where  $\Lambda^*$ ,  $A_\mu$ ,  $Y$ ,  $K$  and  $K^*$  denote the  $\Lambda(1405)$ , photon, hyperon ( $\Sigma$  or  $\Lambda$ ),  $K$  and  $K^*$  fields, respectively. The charge of electron  $e$  and  $\pi$  decay constant  $F_\pi$  are taken as the usual values, i.e.  $e = \sqrt{4\pi/137}$  and  $F_\pi = 92.2 \text{ MeV}$ [16].  $g_c$  describes the coupling strength of the contact term, and we treat it as a free parameter in this work. Other coupling constants in the Lagrangians are taken from previous studies, which are determined by either fitting the experimental data or theoretical predictions. The values for these parameters and relevant references are listed in Table I.

For the strong interaction vertices, the interaction La-

grangian densities can be written as [12, 15]:

$$\mathcal{L}_{KNY} = -ig_{KNY} \bar{N} \gamma_5 Y K + \text{H.c.}, \quad (6)$$

$$\mathcal{L}_{\Lambda^* KN} = -ig_{\Lambda^* KN} \bar{N} \Lambda^* K + \text{H.c.}, \quad (7)$$

$$\mathcal{L}_{\Lambda^* K^* N} = -g_{\Lambda^* K^* N} \bar{N} \gamma_5 \gamma_\mu \Lambda^* K^{*\mu} + \text{H.c.}, \quad (8)$$

$$\mathcal{L}_{\Lambda^* \pi \Sigma} = ig_{\Lambda^* \pi \Sigma} \bar{\Lambda}^* \vec{\pi} \cdot \vec{\Sigma} + \text{H.c.} \quad (9)$$

Here we take the coupling constants  $g_{KN\Lambda}$  and  $g_{KN\Sigma}$  from the Nijmegen soft-core potential[17]. Current knowledge of the  $g_{\Lambda^* K^* N}$  is still rather limited, so we take the value from Ref.[18], where the value of  $g_{\Lambda^* K^* N}$  is obtained by averaging the predictions of various chiral-unitary models(ChUM).

To take into account the internal structure of hadrons, we have introduced form factors in the calculations. In this work, the form factor for intermediate hadrons is taken as [15]

$$F(q, m) = \left( \frac{\Lambda^4}{\Lambda^4 + (q^2 - m^2)^2} \right)^2, \quad (10)$$

where  $q$  and  $m$  are the momentum and mass of the exchanged particles. We take  $\Lambda_M = 2.0 \text{ GeV}$  for meson exchange[12], and fit the  $\Lambda_B$ , i.e. the cutoff parameter for baryon exchange, to the experiment data. The propagators for various particles are adopted as below:

$$G_K(q) = \frac{i}{q^2 - m^2} \quad (11)$$

for  $K$ ,

$$G_{K^*}^{\mu\nu}(q) = -\frac{i(g^{\mu\nu} - q^\mu q^\nu / q^2)}{q^2 - m^2} \quad (12)$$

for  $K^*$ ,

$$G_{N/Y}(q) = \frac{i(\not{q} + m)}{q^2 - m^2} \quad (13)$$

for the nucleon or hyperon and

$$G_{\Lambda^*}(q) = \frac{i(\not{q} + m)}{q^2 - m^2 + im\Gamma(q^2)} \quad (14)$$

for the  $\Lambda(1405)$ , where  $q$ ,  $m$  and  $\Gamma(q^2)$  are the four-momentum, mass and width of the exchanged particles respectively. Here we use an energy-dependent form for the width of  $\Lambda(1405)$ . The energy-dependent form is taken as follows [19]:

$$\Gamma(q^2) = \Gamma_{\pi\Sigma}(q^2) + \Gamma_{\bar{K}N}(q^2), \quad (15)$$

$$\Gamma_{\pi\Sigma}(q^2) = \frac{3g_{\Lambda^* \pi \Sigma}^2 |\vec{p}_{\pi\Sigma}(q^2)|}{4\pi\sqrt{q^2}} \times \left( M_\Sigma + \sqrt{M_\Sigma^2 + |\vec{p}_{\pi\Sigma}(q^2)|^2} \right), \quad (16)$$

$$\Gamma_{\bar{K}N}(q^2) = \frac{2g_{\Lambda^* \bar{K}N}^2 |\vec{p}_{\bar{K}N}(q^2)|}{4\pi\sqrt{q^2}} \theta(\sqrt{q^2} - M_{\bar{K}} - M_N) \times \left( M_N + \sqrt{M_N^2 + |\vec{p}_{\bar{K}N}(q^2)|^2} \right), \quad (17)$$

where  $\vec{p}_{\pi\Sigma}$  or  $\vec{p}_{\bar{K}N}$  denotes the momentum of final particles in the rest frame of  $\Lambda^*$ . Below the  $\bar{K}N$  threshold, the momentum  $\vec{p}_{\bar{K}N}$  is taken as zero.

With the ingredients presented above, the amplitudes for the  $\gamma p \rightarrow K^+\Lambda^*(\rightarrow \pi\Sigma)$  process can be obtained in a standard way, and we get

$$\mathcal{M}_K = 2e g_{\Lambda^*KN} g_{\Lambda^*\pi\Sigma} \bar{u}(p_5, \lambda_\Sigma) G_{\Lambda^*}(q_{\Lambda^*}) p_3 \cdot \epsilon u(p_2, \lambda_p) G_K(q_K) F_{KN}, \quad (18)$$

$$\mathcal{M}_N = e g_{\Lambda^*KN} g_{\Lambda^*\pi\Sigma} \bar{u}(p_5, \lambda_\Sigma) G_{\Lambda^*}(q_{\Lambda^*}) G_N(q_N) \left( \gamma^\mu + \frac{i\kappa_N}{2M_N} \sigma^{\mu\nu} p_{1\nu} \right) \epsilon_\mu u(p_2, \lambda_p) F_{KN}, \quad (19)$$

$$\mathcal{M}_{K^*} = i g_{\gamma KK^*} g_{\Lambda^*K^*N} g_{\Lambda^*\pi\Sigma} \bar{u}(p_5, \lambda_\Sigma) G_{\Lambda^*}(q_{\Lambda^*}) \varepsilon^{\mu\nu\alpha\beta} p_{1\mu} \epsilon_\nu q_{K^*\alpha} G_{\beta\rho}^{K^*}(q_{K^*}) \gamma_5 \gamma^\rho u(p_2, \lambda_p) F_{K^*}, \quad (20)$$

$$\mathcal{M}_Y = \frac{ie\mu_{\Lambda^*Y} g_{KNY} g_{\Lambda^*\pi\Sigma}}{2M_N} \bar{u}(p_5, \lambda_\Sigma) G_{\Lambda^*}(q_{\Lambda^*}) \gamma_5 \sigma_{\mu\nu} \epsilon^\mu p^{1\nu} G_Y(q_Y) \gamma_5 u(p_2, \lambda_p) F_Y, \quad (21)$$

$$\mathcal{M}_C = g_c \frac{e g_{KN\Sigma}}{4\pi^2 F_\pi^3} \bar{u}(p_5, \lambda_\Sigma) \gamma_5 u(p_2, \lambda_p) \varepsilon^{\mu\nu\alpha\beta} p_{1\mu} \epsilon_\nu q_{K\alpha} p_{3\beta} G_K(q_K) F_K, \quad (22)$$

where  $p_i$  represents the four-momentum of the particles as denoted in Fig.1 and  $Y$  denotes  $\Lambda$  or  $\Sigma$ .  $F_{M/B}$  is the form factor considered for meson or baryon. To restore the gauge invariance of the amplitude, we have adopted the approach in Ref.[15] and defined the common form factor as

$$F_{KN} = F_K + F_N - F_K F_N. \quad (23)$$

In previous studies[15], it was shown that in the energy region under study the Regge approach was successful in describing the reaction. Following their works, we also adopt the Regge approach in the present model. To do that, we need to replace the  $t$ -channel meson propagators in the amplitudes with the Regge propagators [15, 20]:

$$\frac{1}{t - M_K^2} \rightarrow \left( \frac{s}{s_0} \right)^{\alpha_K} \frac{\pi \alpha'_K}{\sin(\pi \alpha_K)} \frac{1}{\Gamma(1 + \alpha_K)},$$

$$\frac{1}{t - M_{K^*}^2} \rightarrow \left( \frac{s}{s_0} \right)^{\alpha_{K^*} - 1} \frac{\pi \alpha'_{K^*}}{\sin(\pi \alpha_{K^*})} \frac{1}{\Gamma(\alpha_{K^*})}, \quad (24)$$

where  $t$  denotes the Mandelstam variable, and Regge trajectories read [15]

$$\alpha_K = \alpha_K(t) = \frac{0.7}{GeV^2} (t - M_K^2),$$

$$\alpha_{K^*} = \alpha_{K^*}(t) = \frac{0.83}{GeV^2} t + 0.25. \quad (25)$$

The slope parameter is defined as  $\alpha'_{K,K^*} \equiv \partial \alpha_{K,K^*}(t) / \partial t$ , and the energy scale parameter  $s_0$  is chosen to be 1 GeV<sup>2</sup>[15, 20].

The total amplitude  $\mathcal{M}$  is obtained by the summation of the individual amplitudes. The differential and total

cross sections for this reaction then can be calculated through

$$d\sigma = \frac{1}{8} \frac{m_N}{(2\pi)^5 (p_1 \cdot p_2)} \sum_{\lambda_\gamma \lambda_p \lambda_\Sigma} |\mathcal{M}|^2 \frac{d^3 p_3}{2E_K} \frac{d^3 p_4}{2E_\pi} \frac{M_\Sigma d^3 p_5}{E_\Sigma} \times \delta^4(p_1 + p_2 - p_3 - p_4 - p_5), \quad (26)$$

where  $\lambda_\gamma, \lambda_p, \lambda_\Sigma$  are the helicities of the photon, proton and  $\Sigma$ , respectively.

For the one-pole case, the total amplitude can be represented by

$$\mathcal{M} = \mathcal{M}_K + \mathcal{M}_N + \mathcal{M}_{K^*} + \mathcal{M}_Y + \mathcal{M}_C. \quad (27)$$

TABLE I: Values for the parameters taken from other references.

parameter	value	parameter	value
e	0.303	$\Lambda_M$	2.0GeV[12]
$\kappa_N$	1.79[15]	$g_{\gamma KK^*}$	-0.254/GeV[15]
$g_{KN\Lambda}$	-13.4[17]	$g_{KN\Sigma}$	4.09[17]
$F_\pi$	92.2MeV[16]	$g_{\Lambda^*K^*N}^a$	1.30[18]
$g_{\Lambda^*K^*N}$	1.30[18]	$g_{\Lambda^*_H K^*N}$	3.75[18]
$\gamma_L^b$	0.85[23]	$\gamma_H^b$	2.37[23]

<sup>a</sup>Here we use  $g_{\Lambda^*K^*N}$  to denote the  $\Lambda(1405)\bar{K}^*N$  coupling constant for the one-pole case.

<sup>b</sup>Here we define  $\gamma_{L/H} = g_{\Lambda^*_{L/H}KN} / g_{\Lambda^*_{L/H}\pi\Sigma}$ .

Here the amplitude  $\mathcal{M}_Y$  represents the contribution from the hyperon exchange diagrams(Fig.1(b)). In principle, both the  $\Lambda$  and  $\Sigma$  exchange amplitudes should be taken into account explicitly. While due to the poor knowledge of the  $\Lambda^*Y\gamma$  coupling and the minor role of their contributions in the present reaction, we take the  $\mathcal{M}_Y = \mathcal{M}_\Lambda$  and set  $\mu_{\Lambda^*\Lambda}$  as a free parameter to effectively take into account the sum of their contributions. So in the following discussions, we will not distinguish their individual contributions. To evaluate the amplitudes, the parameters in the amplitudes, such as the coupling constants, cutoff parameters and the parameters of the resonance, need to be determined. In principle, all these parameters need to be determined by fitting to the experimental data. To reduce the number of free parameters, some parameters are fixed with the values obtained in previous studies. As mentioned above, we list the values of the parameters taken from other studies in Table I. For other parameters, we fit them to the data of the  $\gamma p \rightarrow K^+\pi\Sigma$  reaction. Now we have four free parameters, which are three coupling constants( $\mu_{\Lambda^*\Lambda}$ ,  $g_{\Lambda^*\bar{K}N}$ ,  $g_c$ ) and one cutoff parameter( $\Lambda_B$ ). To determine these parameters, we fit them to the recent data from the CLAS collaboration, which include the angular distributions of the  $K^+$ , invariant mass spectrum of the  $\pi\Sigma$  and the polarization data. Note that at center of mass energies larger than 2.3 GeV the  $K^+$  angular distribution or the

$M_{\pi\Sigma}$  spectrum for the three charged channels of the  $\pi\Sigma$  system are similar to each other. Due to the relatively large uncertainties of the data and for simplicity, we use the sum data of the  $\pi^+\Sigma^-$ ,  $\pi^-\Sigma^+$  and  $\pi^0\Sigma^0$  channels for the final analysis as in Ref.[12]. For later convenience, here we define  $\gamma = g_{\Lambda^*KN}/g_{\Lambda^*\pi\Sigma}$ . In the fitting, we set  $\gamma$  as free parameter, and then the  $g_{\Lambda^*KN}$  is determined by the product of the  $\gamma$  and  $g_{\Lambda^*\pi\Sigma}$ . By fitting to the data, the free parameters are determined and presented in Table II. The fitting results for the total cross sections, the angular distributions, the  $\pi\Sigma$  invariant mass spectrum and the  $\Sigma$  polarization are shown by the solid line in Figs. (2)–(5).

TABLE II: Fitted parameters for the one-pole case ( $\chi^2/dof=2.41$ ).

parameter	value	parameter	value
$\Lambda_B$	$2.00 \pm 0.05$ GeV	$\gamma$	$2.36 \pm 0.02$
$\mu_{\Lambda^*\Lambda}$	$0.077 \pm 0.002$	$g_c$	$-8.57 \pm 0.12$

To explore the possible effects due to the two-pole structure of the  $\Lambda(1405)$ , we also need to discuss the formalism for the two-pole case. For the two-pole case, we assume there are two I=0 resonances, i.e.  $\Lambda_L^*$  and  $\Lambda_H^*$ , in the  $\Lambda(1405)$  region, and then the productions of both these two resonances need to be considered in the full amplitude. Here the subscripts  $L$  and  $H$  denote the states corresponding to the low- and high- mass poles of the  $\Lambda(1405)$  respectively. Since the two resonances have same quantum numbers, the Feynman diagrams and the structures of the amplitudes for the two resonances are basically same and can be presented as the forms in Eqs.(18)-(22). The new ingredients mainly come from the number of independent amplitudes and the parameters in the amplitudes. The total amplitude for the two-pole case can be written as

$$\mathcal{M} = (\mathcal{M}_K^L + \mathcal{M}_N^L + \mathcal{M}_{K^*}^L + \mathcal{M}_Y^L) + (\mathcal{M}_K^H + \mathcal{M}_N^H + \mathcal{M}_{K^*}^H + \mathcal{M}_Y^H)e^{i\phi} + \mathcal{M}_C e^{i\phi_c} \quad (28)$$

where  $\phi$  and  $\phi_c$  are introduced to describe the relative phases among the amplitudes for the two resonances and the contact term<sup>1</sup>. Some previous studies show that the relative phase between the two resonance is about  $\pi$ [12, 21, 22]. Therefore, we adopt  $\phi = \pi$  in this work. Since it is difficult to constrain all the parameters by fitting the data of a single reaction, we adopt the ChUM predictions for some of the parameters. The values for these parameters are taken as:  $g_{\Lambda_L^*K^*N} = 1.30$ ,

$g_{\Lambda_H^*K^*N} = 3.75$  [18]<sup>2</sup>,  $\gamma_L = 0.85$  and  $\gamma_H = 2.37$ [23]. Furthermore, for the same reason as the one-pole case, we will also take into account the contribution of hyperon exchanges by considering the effective amplitudes  $\mathcal{M}_{\Lambda}^{L,H}$  with assuming  $\mu_{\Lambda_L^*\Lambda} = \mu_{\Lambda_H^*\Lambda}$ . Other parameters will be fixed by fitting the experiment data.

TABLE III: Fitted parameters for the two-pole case ( $\chi^2/dof=2.13$ ).

parameter	value	parameter	value
$\Lambda_B$	$1.94 \pm 0.09$ GeV	$\mu_{\Lambda_{L/H}^*\Lambda}$	$0.069 \pm 0.006$
$g_c$	$8.35 \pm 0.16$	$\phi_c$	$-0.92 \pm 0.12$
$M_{\Lambda_L^*}$	$1357.9 \pm 1.1$ MeV	$M_{\Lambda_H^*}$	$1425.1 \pm 3.4$ MeV
$g_{\Lambda_L^*\pi\Sigma}$	$1.13 \pm 0.05$	$g_{\Lambda_H^*\pi\Sigma}$	$1.04 \pm 0.07$

## RESULTS AND DISCUSSION

With the help of the cernlib package MINUIT and the formalisms presented in the last section, the free parameters are fitted to the experimental data from the CLAS collaboration[8]. In Fig. 2, we show the total cross sections for the  $\gamma p \rightarrow K^+\pi\Sigma$  reaction as a function of the photon laboratory energy  $E_{lab}$ , where the solid and dashed lines correspond to the results for the one-pole case and two-pole case respectively. As discussed in Sec. I, only the data at the c.m. energies(W) ranging from 2.3 GeV to 2.8 GeV are fitted in this work. While, the comparison between our results and the experimental data at  $W < 2.3$  GeV are also shown for completeness. The significant discrepancy at the near threshold region can be attributed to the ignoring of the  $s$ -channel nucleon resonance contributions. At higher energies, their contributions are expected small[15].

In Tables II and III, we present the fitted parameters for the one-pole and two-pole cases. For the one-pole case, the mass and width of the  $\Lambda(1405)$  have been taken as the values suggested by PDG. The coupling constant  $g_{\Lambda^*\pi\Sigma}$  can be determined through the decay width. While, the coupling constants  $g_{\Lambda^*\bar{K}N}$  will be determined by fitting the experimental data. In literatures, the values for these two coupling constants and their ratio have been intensively studied(see Ref.[24, 25] for a detailed discussion) and our current knowledge about these parameters still has large uncertainties. For example, the ratio of  $g_{\Lambda^*\bar{K}N}$  to  $g_{\Lambda^*\pi\Sigma}$  may vary in a range of 1.6-7.8[19].

<sup>1</sup> It should be noted that a relative phase between the resonance production amplitudes and the contact term can also be introduced in the one-pole case. While, we find the final results are not sensitive to this phase. So the introduction of this phase in the one-pole case will not change the results presented below.

<sup>2</sup> At present, our knowledge of the coupling constants  $g_{\Lambda_{H/L}^*K^*N}$  are still rather limited. Here we adopt one set of values of the  $g_{\Lambda_{H/L}^*K^*N}$  predicted in Ref.[18] in the calculations. While, since the  $K^*$  exchange contribution only plays a minor role in this reaction, if we adopt other predictions for these two coupling constants in Ref.[18] the results will not change significantly.

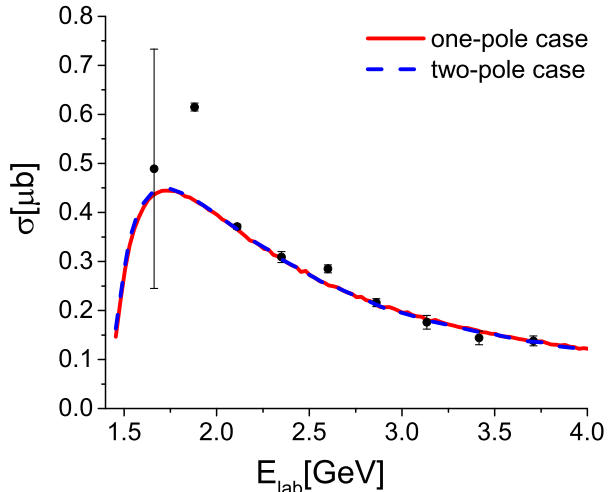


FIG. 2: Total cross sections for the  $\gamma p \rightarrow K^+ \pi \Sigma$  reaction as a function of the photon laboratory energy  $E_{lab}$ . The red-solid and blue-dashed lines indicate the one-pole and two-pole results, respectively. The data are taken from Ref. [8].

We find our fitting results of these coupling constants and their ratio are consistent with previous studies. This may give us some confidence about the reliability of our model. For the two-pole case, the masses of the two resonances are set as free parameters. In the fitting, we find that if no constraint is imposed the fitting will converge on some solutions which is equivalent to the one-pole case. To pick out the solution corresponding to the prediction of the ChUM, we have demanded the masses of the two resonances should satisfy the condition  $M_{\Lambda_L^*} < 1.4$  GeV and  $M_{\Lambda_H^*} > 1.4$  GeV[26]. With this constraint condition, the obtained masses of the two resonances are 1357.9 MeV and 1425.1 MeV, respectively. Using the fitted values for the coupling constants  $g_{\Lambda_L^* \pi \Sigma}$  and  $g_{\Lambda_H^* \pi \Sigma}$ , the decay width of the resonances can be obtained, and we get  $\Gamma_{\Lambda_L^*} = 47$  MeV and  $\Gamma_{\Lambda_H^*} = 75$  MeV.

The fitting results for the angular distribution and the invariant mass spectrum are presented in Figs. 3 and 4. Our results show that in our models both the one-pole and two-pole pictures can give a good description of the data at the energies  $W > 2.3$  GeV. While, at the energies  $W \leq 2.3$  GeV the two-pole picture gives a better description of the invariant mass spectrum, even though only the data with  $W \geq 2.3$  GeV are considered in the fitting. For the angular distributions, the results of the one-pole and two-pole models overlap with each other, which shows that the angular distribution is insensitive to the pole structures of the  $\Lambda(1405)$ . In the angular distributions, the  $t$ -channel  $K$  and  $K^*$  meson exchanges are responsible for the enhancement at forward angles, and the  $u$ -channel hyperon exchange results in the slight enhancement at backward angles.

After a brief discussion of the results of the total cross

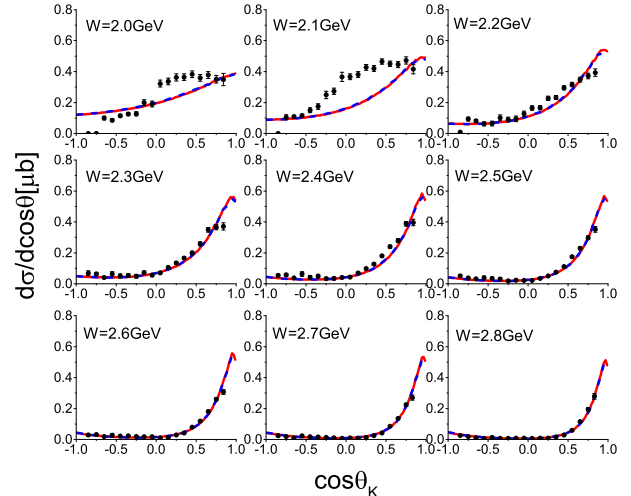


FIG. 3: The angular distributions of the  $K^+$  in the center of mass frame with  $\theta_K$  being the angle between the  $K^+$  momentum and the beam direction. The legends for the lines are the same as those for the Fig. 2. The data are taken from Ref. [8].

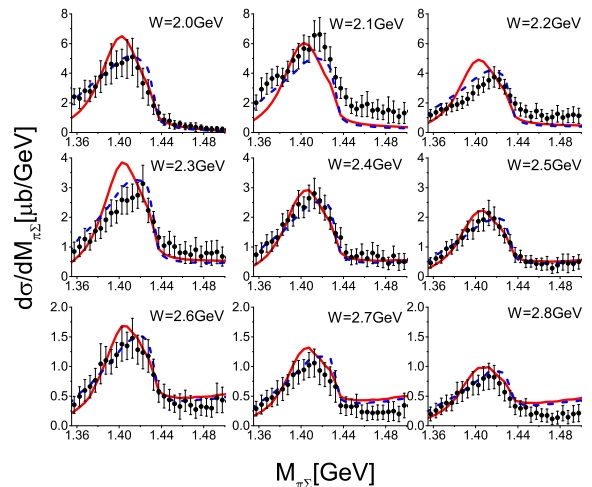


FIG. 4: The invariant mass spectrum of the final  $\pi \Sigma$  system. The legends for the lines are the same as those for the Fig. 2. The data are taken from Ref. [9].

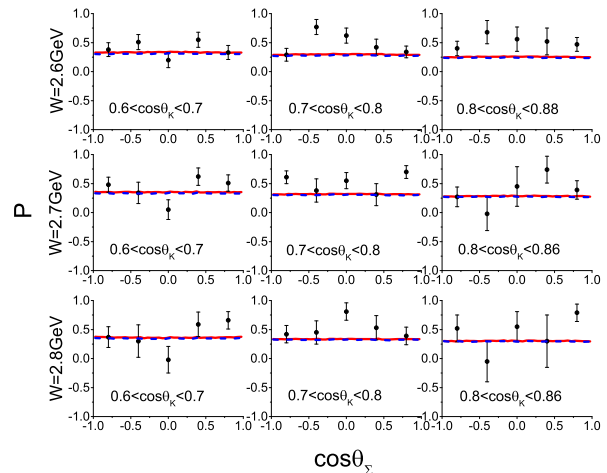
sections, angular distributions and invariant mass spectrums, let us come to the  $\Lambda(1405)$  polarization in this reaction. In Ref.[14], the CLAS collaboration has explored the polarization of the  $\Lambda(1405)$  in the reaction  $\gamma p \rightarrow K^+ \Lambda(1405)$  at  $0.6 < \cos \theta_{K^+}^{c.m.} < 0.9$  in the energy range  $2.55 < W < 2.85$  GeV. Based on some general arguments, they concluded that using an unpolarized beam and target the polarization of the  $\Lambda(1405)$  can only hap-

pen in the direction out of the production plane, and in the process  $\Lambda(1405) \rightarrow \pi + \Sigma$  the polarization of  $\Sigma$  is exactly the same as the polarization of the  $\Lambda(1405)$  in the  $\Lambda(1405)$  rest frame regardless of decay angle if the  $\Lambda(1405)$  is a  $s$ -wave state. Based on their measurement and analysis, they found the experimental data supported the  $s$ -wave nature of the  $\Lambda(1405)$ , which is the first experimental determination of the  $J^P$  quantum numbers of the  $\Lambda(1405)$ . Since the produced  $\Lambda(1405)$  is polarized in the present reaction, it will then be interesting to discuss the mechanism for its polarization. Furthermore, it is also interesting to discuss the possible different predictions of the  $\Lambda(1405)$  polarization in the one-pole or two-pole pictures of the  $\Lambda(1405)$ . To our best knowledge, such questions are still not discussed in previous works[10–13].

First, we tried to reproduce the polarization data by only considering the  $\Lambda(1405)$  production amplitudes(Fig.1a-1c). In such a model, we can describe the angular distribution and the invariant mass spectrum well as in Ref.[15]. However, the polarization data can not be reproduced. We then introduce a contact term(Fig.1d) in the present model. After including the contact term contribution, now we can interpret the  $\Sigma$  polarization data well. As shown in Fig. 5, the polarization of  $\Sigma$  is almost flat in the  $\Lambda^*$  rest frame with the polarization axis being along the direction out of the production plane, which is consistent with the  $s$ -wave nature of the  $\Lambda(1405)$ . As can be seen from the figures, our result agrees well with the current experiment data. We also find that both the one-pole and two-pole pictures can give a good description of the polarization data. It is then interesting to ask whether one can find some observable to distinguish the one- or two-pole models in a single reaction. As we know, the distinct feature of the two-pole picture is that the two poles are near and may have different coupling strengths to  $\pi\Sigma$  and  $\bar{K}N$  channels. It is then natural to expect that the strengths of the contributions of the two poles are different and their relative roles may change as the invariant mass  $M_{\pi\Sigma}$  crosses the  $\Lambda(1405)$  region. Since the polarization observables are sensitive to the interference term and thus the change of the relative roles of the two poles, it is possible that the polarization of  $\Lambda(1405)$ (or more accurately, the polarization of the  $\Sigma$ ) may have a quite different dependence on the invariant mass  $M_{\pi\Sigma}$  in the one-pole and two-pole pictures.

In Fig.6, we study the polarization of the final  $\Sigma$  versus  $M_{\pi\Sigma}$  at some angle bins<sup>3</sup>. It is found the polarization of

the  $\Sigma$  indeed shows different patterns in the  $\Lambda(1405)$  region for the two pictures. Through a more detailed study, we find the  $\Sigma$  polarization originates from the interference between the  $\Lambda(1405)$  production amplitude and the contact term, and the polarization is sensitive to their relative phases. If the two-pole picture is correct, the relative roles of the two poles may change in the  $\Lambda(1405)$  region, which may result in a strong dependence of the  $\Sigma$  polarization on the  $M_{\pi\Sigma}$ . In Fig.7 we present the contributions of the  $\Lambda_L^*$ , the  $\Lambda_H^*$  and the contact term in the invariant mass spectrum at the same angle bins as in Fig.6. It is found that the  $\Sigma$  polarization may show strong dependence on the  $M_{\pi\Sigma}$  at the place where the contributions of the two resonances are comparable. Here we need to note that the pattern of the  $\Sigma$  polarization shown in Fig.6 is dependent on the relative phase between the two resonances, which is set as  $\phi = \pi$  in this work. By adopting a different value for  $\phi$ , the pattern of the  $\Sigma$  polarization will change. However, the strong dependence of the  $\Sigma$  polarization on the  $M_{\pi\Sigma}$  remains at the place where the two resonances have comparable contributions<sup>4</sup>. Therefore, we expect the measurement of the  $\Sigma$  polarization versus the invariant mass  $M_{\pi\Sigma}$  in the  $\gamma p \rightarrow K^+\Lambda(1405)$  reaction may offer the chance to verify the pole structure of the  $\Lambda(1405)$ .



<sup>3</sup> It is worth noting that the  $\Sigma(1385)$  and the  $K^*(892)$  also contribute in this reaction. For the  $\Sigma(1385)$ , due to its small coupling to the  $\pi\Sigma$  channel and its weak interferences with other contributions, it only plays a minor role here. We have checked that in our model the inclusion of the  $\Sigma(1385)$ 's contribution does not significantly change the results presented below. The  $K^*(892)$ 's contribution is not considered because it also plays a minor role in this reaction[27]. Furthermore, at the energies con-

sidered in this work the bands of the  $K^*(892)$  and the  $\Lambda(1405)$  are well separated in the Dalitz plot[14]. So it is possible to eliminate its contribution by a cut on the invariant mass of the  $K\pi$  system. After a cut on the  $K^*(892)$ 's contribution, it will be safe to ignore its contribution and the effects due to its finite width on the results presented below.

<sup>4</sup> In this work, we have also tried to set  $\phi$  as 0,  $\pi/2$  or  $3\pi/2$ . In these cases, the strong dependence of the  $\Sigma$  polarization on the  $M_{\pi\Sigma}$  remains. However, we can not get a good description of the invariant mass spectrum.

FIG. 5: The polarization of the final  $\Sigma$  as a function of  $\cos\theta_\Sigma$  in the rest frame of  $\pi\Sigma$  for the chosen kinematic bins. The polarization axis is taken along  $\vec{p}_\gamma \times \vec{p}_{K^+} / |\vec{p}_\gamma \times \vec{p}_{K^+}|$  and the  $\theta_\Sigma$  is defined as the angle between the  $\Sigma$  momentum and the polarization axis. The legends for the lines are the same as those for the Fig. 2. The data are taken from Ref. [14].

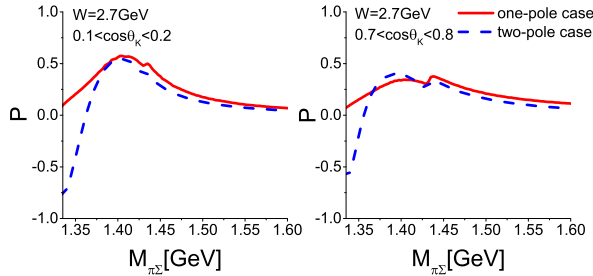


FIG. 6: The polarization of  $\Sigma$  as a function of  $M_{\pi\Sigma}$  at the c.m. energy  $W = 2.7$  GeV for  $0.1 < \cos\theta_{K^+}^{c.m.} < 0.2$  and  $0.7 < \cos\theta_{K^+}^{c.m.} < 0.8$ .

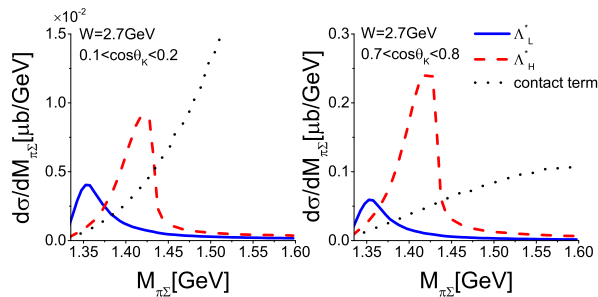


FIG. 7: The contributions of the  $\Lambda_L^*$ ,  $\Lambda_H^*$  and contact term in the  $M_{\pi\Sigma}$  spectrum at the c.m. energy  $W = 2.7$  GeV for  $0.1 < \cos\theta_{K^+}^{c.m.} < 0.2$  and  $0.7 < \cos\theta_{K^+}^{c.m.} < 0.8$ .

Based on the above discussions, we conclude that our model results show the measurement of the  $\Sigma$  polariza-

tion versus  $M_{\pi\Sigma}$  may verify the two-pole picture of the  $\Lambda(1405)$  predicted by the ChUM. Until now, there is still no final conclusion about this issue. So it is important to find some new way to distinguish the two pictures of the  $\Lambda(1405)$ . Although the results presented above may have model dependence, the argument about the different dependence of the  $\Sigma$  polarization on the  $M_{\pi\Sigma}$  in the two pictures may also hold for other models. Since the polarization observable is more sensitive to the interference terms among the amplitudes, we expect the polarization observable may offer more clues about the pole structure of the  $\Lambda(1405)$ . Furthermore, we also expect that a similar conclusion can be made for other  $\Lambda(1405)$  production processes, where the produced  $\Lambda(1405)$  is polarized.

## SUMMARY

In this work, we investigate the polarization of the  $\Lambda(1405)$  in the  $\gamma p \rightarrow K^+ \pi \Sigma$  reaction. We consider the contributions from the t-channel  $K/K^*$  exchanges, the u-channel hyperon exchange and a contact term. In our model, the contact term is necessary for interpreting the  $\Lambda(1405)$  polarization. In addition, we also find that although both the one-pole and two-pole models can give a good description of the angular distribution and the invariant mass spectrum data, they give distinct predictions for the polarization of the final  $\Sigma$  versus the  $M_{\pi\Sigma}$ . Thus the measurement of the dependence of the  $\Sigma$  polarization on the  $M_{\pi\Sigma}$  can offer valuable information about the pole structure of the  $\Lambda(1405)$ . To make this measurement, a large statistics of data will be needed. We hope such a measurement can be done in the future.

## Acknowledgments

We acknowledge the support from the National Natural Science Foundation of China under Grants No.U1832160 and No.11375137, the Natural Science Foundation of Shaanxi Province under Grant No.2019JM-025, and the Fundamental Research Funds for the Central Universities.

- 
- [1] R. Dalitz and S. Tuan, Phys. Rev. Lett. **2**, 425-428 (1959).
  - [2] R. Dalitz and S. Tuan, Annals Phys. **10**, 307-351 (1960).
  - [3] N. Isgur and G. Karl, Phys. Rev. **D 18**, 4187 (1978).
  - [4] P. Fink, Jr., G. He, R. Landau and J. Schnick, Phys. Rev. **C 41**, 2720-2725 (1990).
  - [5] J. Oller and U. G. Meissner, Phys. Lett. **B 500** (2001) 263.
  - [6] E. Oset, A. Ramos and C. Bennhold, Phys. Lett. **B 527** (2002) 99.
  - [7] D. Jido, J. A. Oller, E. Oset, A. Ramos and U. G. Meissner, Nucl. Phys. **A 725** (2003) 181.
  - [8] K. Moriya, *et al.*, [CLAS Collaboration], Phys. Rev. **C 88**, (2013) 045201.
  - [9] K. Moriya, *et al.*, [CLAS Collaboration], Phys. Rev. **C 87**, (2013) no.3, 035206.
  - [10] S. X. Nakamura and D. Jido, PTEP **2014** (2014) 023D01.
  - [11] L. Roca and E. Oset, Phys. Rev. **C 87** (2013) no.5, 055201.
  - [12] S. i. Nam and H. K. Jo, arXiv:1503.00419 [hep-ph]

PKNU-NUHATH-2015-02.

- [13] E. Oset and L. Roca, EPJ Web Conf. **97** (2015) 00023.
- [14] K. Moriya, *et al.*, [CLAS Collaboration], Phys. Rev. Lett. **112** (2014) no.8, 082004.
- [15] S. H. Kim, S. i. Nam, *et al.*, Phys. Rev. **D 96** (2017) no.1, 014003.
- [16] M. I. Vysotsky and E. V. Zhemchugov, Phys. Rev. **D 93** (2016) no.9, 094029.
- [17] V. G. J. Stoks and T. A. Rijken, Phys. Rev. **C 59** (1999) 3009.
- [18] K. P. Khemchandani, A. Martinez Torres, *et al.*, Phys. Rev. **D 84** (2011) 094018.
- [19] J. J. Xie, B. C. Liu and C. S. An, Phys. Rev. **C 88** (2013) no.1, 015203.
- [20] X. Y. Wang and J. He, Eur. Phys. J. **A 55** (2019) no.9, 152.
- [21] R. A. Schumacher and K. Moriya, Nucl. Phys. **A 914** (2013) 51.
- [22] R. Molina and M. Döring, Phys. Rev. **D 94** (2016) no.5, 056010.
- [23] S. I. Nam, *et al.*, J. Korean Phys. Soc. **45** (2004) 1466.
- [24] O. Braun *et al.*, Nucl. Phys. **B 129** (1977), 1-18.
- [25] M. Gell-Mann, R. J. Oakes and B. Renner, Phys. Rev. **175** (1968), 2195-2199.
- [26] L. Roca, J. Nieves and E. Oset, JPS Conf. Proc. **17** (2017) 071002.
- [27] K. Moriya, PhD Thesis, (2010), [http://www.jlab.org/Hall-B/general/thesis/Moriya\\_thesis.pdf](http://www.jlab.org/Hall-B/general/thesis/Moriya_thesis.pdf).